Climate change in the circum-North Atlantic region during the last deglaciation

Jonathan T. Overpeck*, Larry C. Peterson†, Nilva Kipp‡, John Imbrie‡ & David Rind§

* Lamont-Doherty Geological Observatory of Columbia University, Palisades, New York 10964, USA
† Rosenstiel School of Marine and Atmospheric Science, University of Miami, 4600 Rickenbacker Causeway, Miami, Florida 33149, USA
‡ Department of Geological Sciences, Brown University, Providence, Rhode Island 02912, USA
§ NASA Goddard Institute for Space Studies, 2880 Broadway, New York 10025, USA

A survey of new and published palaeoclimate data indicates that both the high- and low-latitude North Atlantic regions were characterized by at least three synchronous periods of abrupt climate change during the last glacial-to-interglacial transition. Climate model results suggest that changes in the melting history of the Laurentide Ice Sheet may explain much of this nonlinear response of the climate system to astronomical (Milankovitch) forcing.

ASTRONOMICAL or Milankovitch forcing has become established as the primary 'pacemaker' of the ice ages, accounting for much of the total observed climatic variance of the late Quaternary[1,2]. Most climatic variance at frequencies lower than 1 cycle per 19,000 years is related to astronomical forcing, and even abrupt glacial terminations can be partially attributed to such forcing[3]. A closer look at the last glacial–interglacial transition, however, reveals a sequence of climate change that cannot be explained as a simple linear response to astronomical forcing. Marine and terrestrial records of environmental change in the high-latitude North Atlantic, Greenland and Europe reveal a period of rapid climatic warming at ~13–12.6 kyr BP, followed by an abrupt reversal towards colder glacial conditions at ~11 kyr, and a second rapid warming to interglacial conditions at ~10 kyr (refs 4–7). The abrupt 13-kyr warming and the 'Younger Dryas' cold event between 11 and 10 kyr were apparently more pronounced over Greenland and Europe than over North America, an observation that has led workers to surmise that changes in the heat budget of the high-latitude North-Atlantic produced the changes over land[5–9]. Ruddiman[4] proposed that a reduction in ice-sheet height over North America could have rapidly reduced the amount of cold air advected over the North Atlantic, thus allowing the North Atlantic and downstream Europe to warm abruptly at ~13 kyr. Ruddiman[4] and Broecker *et al.*[5] expanded on earlier work[10–13] to suggest that major diversions of Laurentide Ice Sheet meltwater between the Mississippi and St Lawrence rivers may have caused the North Atlantic, Greenland and Europe to cool at the beginning of the Younger Dryas period (~11 kyr) and then warm abruptly at the end of the Younger Dryas period (~10 kyr). General Circulation Model (GCM) results support the dominant role of North Atlantic sea surface temperature (SST) fluctuations in forcing high-latitude climate change[6,9].

Here we try to place the observed high-latitude pattern of climate change into a more global perspective. First, we examine new and published data from the Caribbean and Gulf of Mexico region that also point to systematic patterns of abrupt change at ~13–12.6, 11 and 10 kyr. We then examine new and published climate model results which suggest that much of the low-latitude pattern of change can be linked to variations in meltwater discharge down the Mississippi and St Lawrence rivers, and the sea surface temperatures of the high-latitude North Atlantic and Gulf of Mexico. Our results lead us to speculate that rapid climate events over Africa may also have been related to these same variations. We conclude with the hypothesis that the climate system translated the relatively gradual astronomical forcing, characteristic of the past 18 kyr, into an inter-related sequence of abrupt climate events over an extensive area of the globe.

Caribbean and Gulf of Mexico regions

In this section, we look at the patterns and sequence of climate change which occurred around the Caribbean and Gulf of Mexico during the last deglaciation. In particular, we focus our initial attention on data derived from an investigation of sediments from the Cariaco Basin (10°40′ N, 65° W), a small (160 × 40 km), deep (1,400 m) anoxic marine basin aligned along the northern continental margin of Venezuela. This margin is

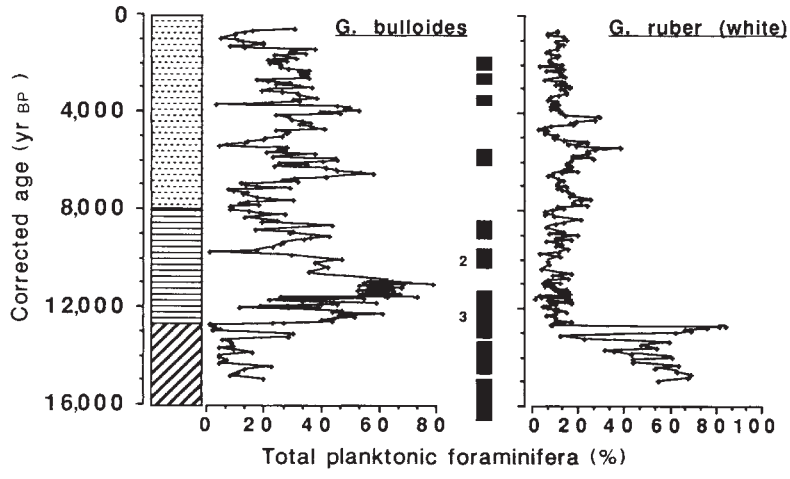

FIG. 1 Time series of *G. bulloides* and *G. ruber* relative abundance for core V12-99 from the Cariaco Basin. Also shown are core lithology and the distribution of radiocarbon-dated intervals which were biostratigraphically correlated from the closely matching, but less continuous, core V12-104. This series of dates did not include any reversals. All dates were adjusted by 400 years to correct for the difference between surface water and atmosphere radiocarbon content. The V12-104 record is less continuous due to the presence of turbidites that were not present in V12-99. ■, radiocarbon-dated intervals (2, 3 = number of dates); Sediment type: ▤, weakly laminated calcareous clays; ▤, strongly laminated calcareous clays; ▨, weakly bioturbated calcareous clays.

currently characterized by Ekman-induced coastal upwelling, with cold SSTs found during the dry winter/spring season of greatest along-shore wind stress, and warmer SSTs during the less windy wet summer season[14,15]. Plankton tow data from the Cariaco Basin indicate that seasonally high abundances of phytoplankton (mainly diatoms) and the planktonic foraminifer *Globigerina bulloides* dominate the water-column assemblage during the upwelling season, whereas *Globigerinoides ruber* is abundant during the non-upwelling season[16].

The strong seasonality in the wind-induced coastal upwelling is reflected in the faunal and lithological character of the laminated sediments which accumulate rapidly (20–100 cm kyr^{-1}) beneath anoxic waters in many portions of the Cariaco Basin. Piston cores V12-99 (1,005 m water depth) and V12-104 (466 m) were sampled on average every 3 and 1 cm, respectively, for a complete foraminiferal census. Age control is provided by twelve radiocarbon dates on bulk carbonate (Fig. 1). We subtracted 400 years from each date to account for the difference in radiocarbon content between the surface waters and atmosphere[5]. The two piston cores, separated by over 50 km, yielded nearly identical time series of foraminiferal abundance, indicating that our faunal records are probably representative of the basin as a whole. We focus here on the abundance record of *G. bulloides* in V12-99 as a proxy record of upwelling, and hence trade-wind intensity (Fig. 1). We will elaborate further on the very detailed Cariaco Basin record elsewhere. Like the high-latitude records of climatic change, the Cariaco Basin record shows evidence of rapid change at ~13–12.6, 11 and 10 kyr.

The presence of weakly bioturbated sediments, the high abundance of *G. ruber*, and the low abundance of *G. bulloides* near the base of the core (Fig. 1) suggest that lowered sea level may have isolated the Cariaco Basin sufficiently to prevent active Ekman-pumping during the last glacial maximum. At 12.6 kyr, both cores record a significant increase in sedimentation rate, an abrupt change from bioturbated to distinctly laminated anoxic sediments (traceable over the entire basin), and a sudden shift in foraminiferal assemblages from a non-upwelling fauna to samples dominated by *G. bulloides*. High concentrations of *G. bulloides* during the period 12.6–10.8 kyr (>2,000 individuals g^{-1} compared to a core mean of <500) suggest that the high sedimentation rates observed throughout this period (>80 cm kyr^{-1} compared to the core mean of <40) were related to intense upwelling and high productivity of *G. bulloides*. The abundance of *G. bulloides* drops abruptly after 10.8 kyr, but remains at levels above the Holocene mean. This change suggests that upwelling and trade-wind intensities, although diminished, were still high during the period 10.8–10 kyr. A further decline in the abundance of *G. bulloides* after 10 kyr suggests that the Holocene mode of moderate (although still highly variable) upwelling began at this time.

The Cariaco Basin upwelling record provides evidence for rather abrupt changes in trade-wind strength at ~12.6, 10.8 and 10 kyr, with the strongest trade winds over the southern Caribbean found between 12.6 and 10.8 kyr. Independent palaeoclimate data from the region support the abrupt nature of change at these times. In the lowlands adjacent to the Caribbean, pollen and lake-level records indicate that glacial (18 kyr) aridity persisted until shortly after 11 kyr, when moist conditions suddenly prevailed[17–19]. To the north of the Gulf of Mexico and Caribbean region, the deglacial sequence of climate change is less clear.

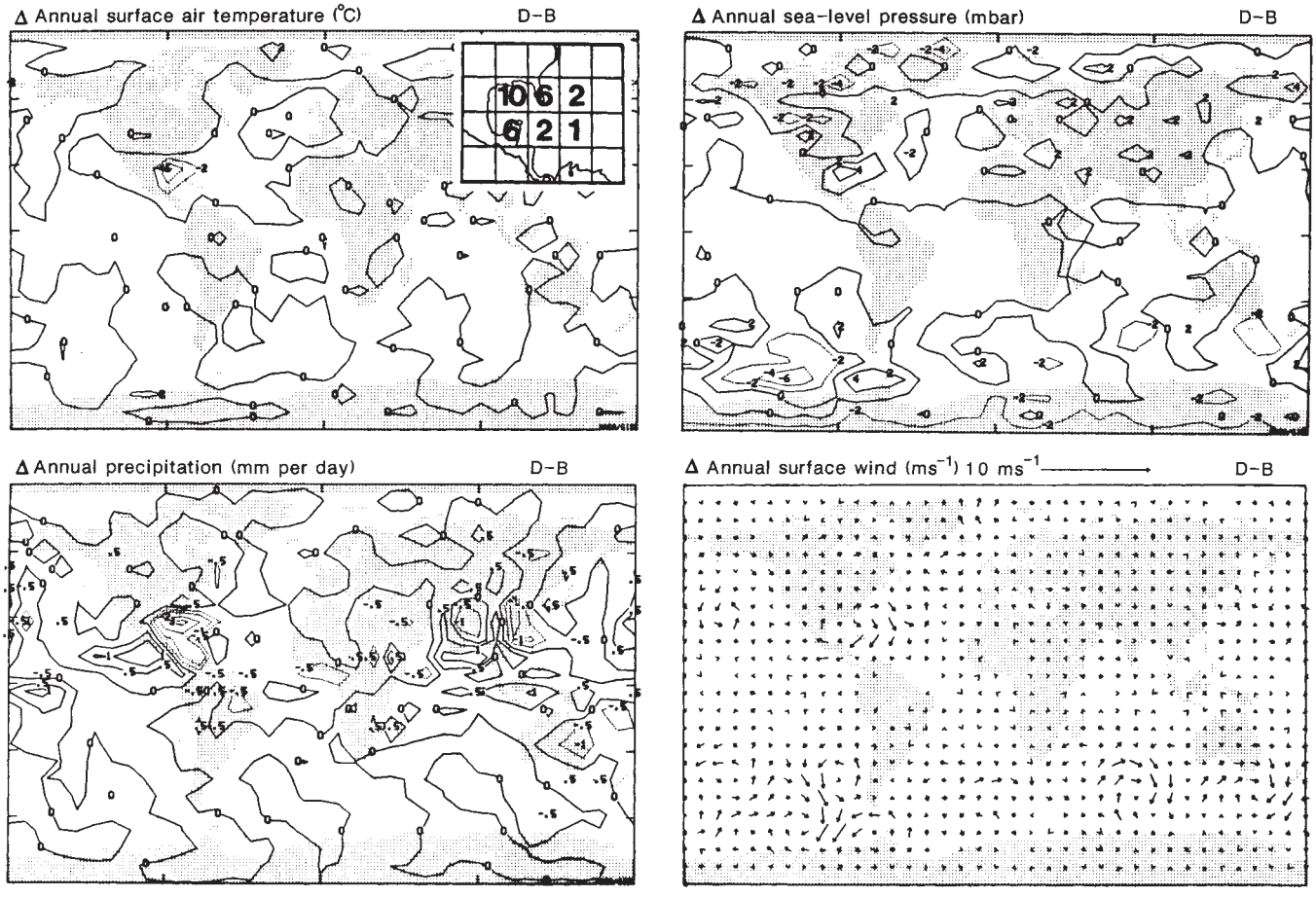

FIG. 2 Simulated mean-annual differences between experiment D and B. Inset shows the magnitude of the negative (°C) SST anomalies (relative to the present-day) that were prescribed for six model grid points in experiment D (see Table 1 and text for more details).

Water levels in low-elevation lakes throughout the southeast US Coastal Plain were low or lakes were dry from before 18 kyr until after 15 kyr, when lake levels rose in response either to increased precipitation, rising sea level, or both[20]. A similarly equivocal record of past hydrological change in this region is the poorly dated record of fluvial changes which seems to indicate moist conditions until 13 kyr (refs 21, 22). Pollen records from the southern Coastal Plain[20,23-27] show abrupt change at 13 and 11 kyr. Increased amounts of herb pollen and decreased abundances of *Carya* pollen may argue for aridity between 13 and 11 kyr in Florida[20,23,24], just as increased amounts of *Fagus* and *Liquidambar* pollen may have signalled the onset of wetter conditions after 11 kyr further north[25-27]. More data are clearly required, however, to refine this regional picture.

Observed versus simulated palaeoclimatic change

The apparent synchroneity between events in the Cariaco Basin record, in other records from the Caribbean and Gulf of Mexico region, and in records from the high-latitude North Atlantic suggest a common forcing mechanism during deglaciation. In particular, the evidence for stronger trade winds between 12.6 and 10.8 kyr in the western North Atlantic and for Gulf/Caribbean aridity until ~11 kyr have led us to examine the effects that a cool Gulf of Mexico may have had on the climate system. Geological data from North America and stable isotope data from Gulf sediments suggest that the flow of cold, fresh Laurentide Ice Sheet meltwater down the Mississippi River and into the Gulf of Mexico began at ~15-14 kyr, waned slightly from ~14-13 kyr, and peaked between 13 and 11 kyr before being diverted down the St Lawrence River into the high-latitude North Atlantic[5,9-12]. During the interval of maximum discharge into the Gulf, which coincides closely with the timing of events described above, the volume of Mississippi outflow must have been immense (5-11 times the present annual discharge, but mostly confined to the spring-summer meltwater season[13,28]), apparently included seasonal ice-rafted detritus (R. Saucier, personal communication), and was sufficient to affect sea surface salinities well out into the western North Atlantic[13,29]. Unlike the role of salinity, little attention has been paid to the possible consequences of meltwater-induced temperature change in the Gulf of Mexico. Independent data[30,31] suggest that the open south-west Caribbean did not warm from glacial values until ~11 kyr, and it seems likely that the more northerly Caribbean and Gulf of Mexico regions may have been cooled even further by the large influx of glacial meltwater. We suggest that cooler Gulf SSTs during peak meltwater discharge could provide a mechanism for explaining observed events if the cooling was sufficient to produce a high regional surface-pressure anomaly, which would in turn strengthen western Atlantic trade winds and suppress precipitation.

To test this hypothesis, we compared the results from four GCM (8° × 10° latitude by longitude grid size) experiments (for details, see Table 1) using the Goddard Institute for Space Studies model[6,32]. Experiment A represents our model simulation of the current (warm) climate. The results of the four-year experiments, B and C, were compared to test the sensitivity of the global climate system to the hypothesized Younger Dryas (~11-10 kyr) reduction in North Atlantic SSTs[6]. We also ran a two-year experiment (D) to test the sensitivity of the climate system to cooled Gulf of Mexico SSTs during the period ~13-11 kyr. Experiment D was identical to B, except that model grid points which included the Gulf of Mexico and adjacent water were cooled by ~6 °C on average (Fig. 2). Unfortunately, the palaeoceanographic record provides no direct evidence for cooling of the Gulf by meltwater. However, the oxygen isotope record of meltwater[10,11,13,29] is useless in this regard because of the predominance of salinity effects, and existing microfossil-based studies of Gulf SSTs[33,34] have sample spacings that may preclude recognition of such a brief (2-kyr) event. In the absence of data to the contrary, we selected an average cooling of 6 °C based on estimates of meltwater volume, on the observation that present-day Mississippi River water is up to 10 °C colder than Gulf surface waters[28,35], and on the observation that downstream Caribbean SSTs were probably already depressed by 2-3 °C before they warmed at 11 kyr to Holocene levels[30,31]. Independently, Oglesby *et al.*[28] have arrived at a similar estimate and, more importantly, have performed sensitivity tests which suggest that an even smaller cooling could still have forced the same patterns of change around the Gulf that we have forced with our SST anomaly.

Our simulated cooling of the Gulf of Mexico (D minus B) produced lower surface air temperatures, higher sea-level pressure, a large negative precipitation anomaly, and a more vigorous anticyclonic surface air circulation over the Gulf of Mexico and Caribbean region (Fig. 2). Each of these changes is statistically significant (greater than several standard deviations of the interannual changes found in experiment B) and agrees with the palaeoclimatic data described in the previous section. The simulated difference between experiments D and A indicate that a cool Gulf of Mexico between ~13 and 11 kyr is needed to match the palaeoclimatic evidence for greater than present aridity around the Gulf and Caribbean region, and more intense trade winds in the western North Atlantic. Averaged over the annual cycle, the cooling of the Gulf produced no significant temperature anomalies outside the Gulf/Caribbean region. In our experiment, the well-developed higher pressure and cooler temperatures in the Gulf region helped divert storm tracks northward, resulting in both lower pressure and a small band of increased precipitation north of the Gulf Coastal Plain. This pattern agrees with the observation that aridity may have been restricted to Florida and Georgia between ~13 to 11 kyr. Slightly higher precipitation values, probably indicative of increased Hadley circulation, were also simulated equatorward of the Gulf of Mexico over the northern Amazon Basin and central Andes. These changes were not as significant (less than three standard deviations) as those simulated around the Gulf of Mexico and Caribbean region, but they do appear to agree with the sparse palaeoclimate data from South America[36,37].

Rind *et al.*[6] compared C and B to demonstrate the importance of high-latitude North Atlantic SSTs in forcing the observed climate changes over North America, Greenland and Europe during the last glacial-interglacial transition. Our comparisons of D with B (Fig. 2) and C with D (Fig. 3) support this conclusion. On a yearly average basis, the observed high-latitude variations in both precipitation and temperature appear to be explained by the observed changes in high-latitude SSTs: rapid warming at ~13 kyr, rapid cooling at ~11 kyr (the onset of the Younger Dryas) and rapid warming again at ~10 kyr (the end of the Younger Dryas). At lower latitudes, the warming of the Gulf at ~11 kyr can explain the wetter conditions and slight wind relaxation observed at this time in the western North Atlantic/Gulf/Caribbean region (Fig. 3). The magnitude of the

TABLE 1 Summary of General Circulation Model experiments

Designation	Description
A	current climate[32]
B	11 kyr orbital parameters[50] 11 kyr land ice[49] current sea surface temperatures
C	11 kyr orbital parameters[50] 11 kyr land ice[49] current sea surface temperatures, except in the North Atlantic north of 25° N where they were cooled to their ice age values (18 kyr)[51]
D	11 kyr orbital parameters[50] 11 kyr land ice[49] current sea surface temperatures, except in the Gulf of Mexico region where they were cooled on average 6 °C (see Fig. 2)

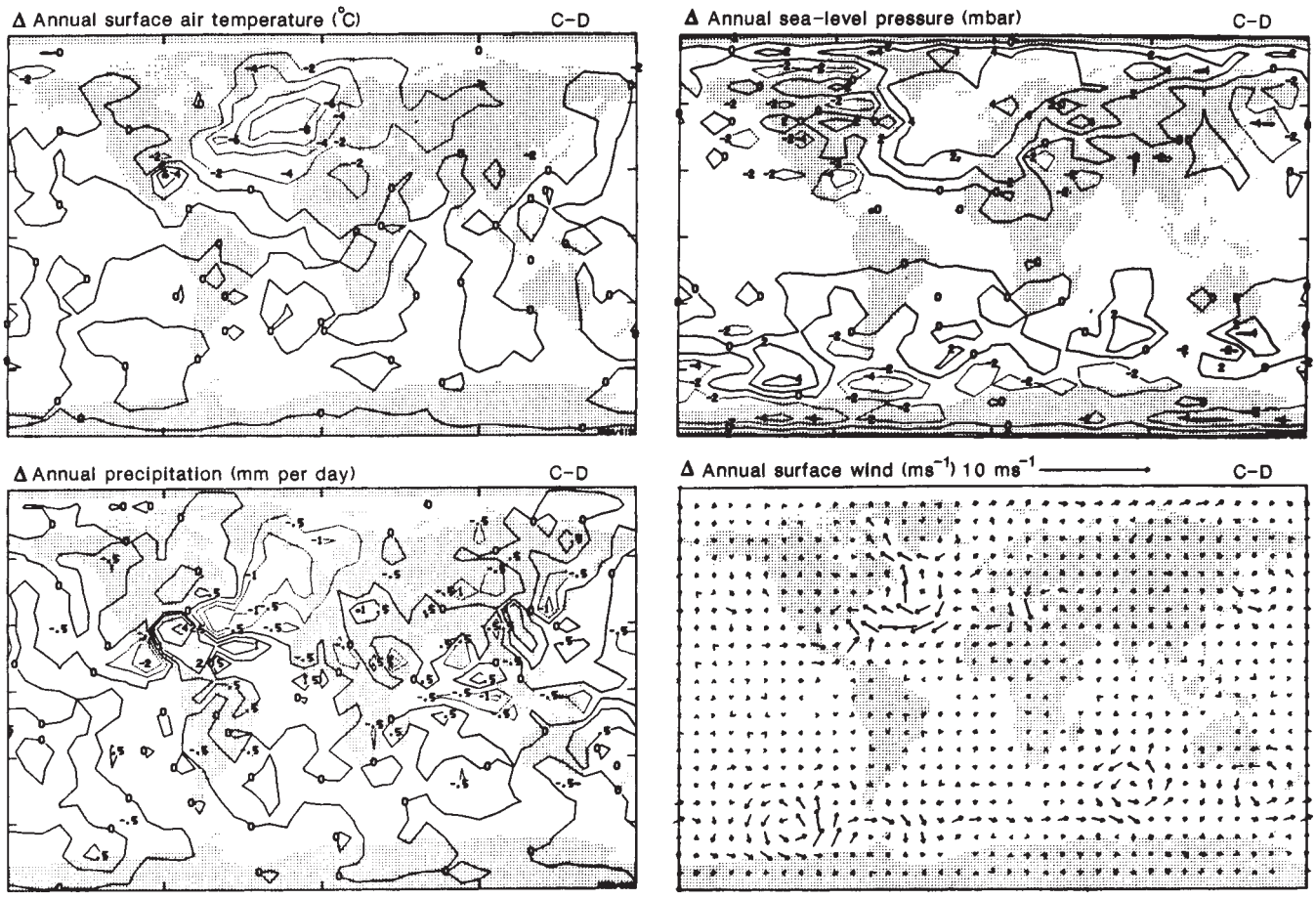

FIG. 3 Simulated mean-annual differences between experiment C and D (see Table 1 and text for more details).

Gulf/Caribbean aridity probably would have been enhanced between 13 and 11 kyr had we prescribed colder SSTs along the northern South American margin in accordance with the Cariaco Basin upwelling record.

Our simulations suggest that the observed pattern of climate change over most of the circum-North Atlantic region can be explained by the proposed effects of cold Laurentide Ice Sheet meltwater on SSTs of the high-latitude North Atlantic and Gulf of Mexico. Our model results may not, however, provide a complete physical explanation for the sequence of change observed over North Africa, and, in particular, for the arid event that apparently was synchronous with the Younger Dryas in Europe (~11-10 kyr, refs 38-46). The increased surface pressure and stronger easterly surface winds in experiment C relative to D (Fig. 3) support the idea[39,44] that a colder North Atlantic could have stabilized the lower atmosphere and helped block the advection of moisture over North Africa. However, the simulated precipitation changes between the two experiments are somewhat ambiguous (Fig. 3). Additional experiments are needed to examine the significance of the precipitation anomalies in East and North Africa. It is also necessary to test the possibility that abrupt changes of high-latitude North Atlantic SSTs were associated with other rapid changes that could have contributed to the observed changes over North Africa. Higher atmospheric aerosols[47], changes in vegetation, a weaker monsoon, and lower-latitude Atlantic SST cooling[48] may all have helped to make North Africa more arid before ~13-12.6 kyr, and between 11 and 10 kyr.

Conclusion

Our postulated synchroneity of rapid climate events at ~13-12.6, 11 and 10 kyr around the circum-North Atlantic must be tested by means of the acquisition of additional well-dated, high-resolution palaeoclimate records. In most cases, we were forced to use dates with an uncertainty of ~5-10% to infer synchroneity. In addition, further efforts to evaluate the palaeotemperature record from the Gulf of Mexico are clearly warranted. These palaeoclimatic studies will have to be augmented by additional climate model experiments to understand the sensitivity of the global climate system to deglacial changes in boundary conditions. Our present simulations, however, support a scenario through which the climate system (via the melting history of the Laurentide Ice Sheet) could have transformed relatively gradual and monotonic astronomical forcing into a series of abrupt, non-monotonic climate changes over a large part of the globe. □

Received 12 December 1988; accepted 17 March 1989.

1. Hays, J. D., Imbrie, J. & Shackleton, N. J. *Science* **194,** 1121-1132 (1976).
2. COHMAP members *Science* **241,** 1043-1052 (1988).
3. Imbrie, J. in *Abrupt Climatic Change—Evidence and Implications* (eds Berger, W. H. & Labeyrie, L. D.) 365-367 (Reidel, Dordrecht, 1987).
4. Ruddiman, W. F. in *North America and Adjacent Oceans During the Last Deglaciation* (eds Ruddiman, W. F. & Wright, H. E. Jr) 463-478 (Geological Society of America, Boulder, 1987).
5. Broecker, W. S. *et al. Paleoceanography* **3,** 1-19 (1988).
6. Rind, D., Peteet, D., Broecker, W., McIntyre, A. & Ruddiman, W. *Clim. Dyn.* **1,** 3-33 (1986).
7. Duplessy, J. C., Delibrias, G., Turon, J. L., Pujol, C. & Duprat, J. *Palaeogeogr., Palaeoclimatol., Palaeoecol.* **35,** 121-144 (1981).
8. Broecker, W. S., Peteet, D. M. & Rind, D. *Nature* **315,** 21-26 (1985).
9. Schneider, S. H., Peteet, D. M. & North G. R. in *Abrupt Climatic Change—Evidence and Implications* (eds Berger, W. H. & Labeyrie, L. D.) 399-417 (Reidel, Dordrecht, 1987).
10. Kennett, J. P. & Shackleton, N. J. *Science* **188,** 147-150 (1975).
11. Leventer, A., Williams, D. F. & Kennett, J. P. *Mar. Geol.* **53,** 23-40 (1983).
12. Teller, J. T. in *North America and Adjacent Oceans During the Last Deglaciation* (eds Ruddiman, W. F. & Wright, H. E. Jr) 39-69 (Geological Society of America, Boulder, 1987).
13. Emiliani, C., Rooth, C. & Stipp, J. J. *Earth planet. Sci. Lett.* **41,** 159-162 (1978).
14. Febres-Ortega, G. & Herrera, L. E. *Bol. Inst. Oceanogr. Univ. Oriente* **14,** 3-29 (1975).
15. Aparicio, R. thesis, Florida Inst. Tech. (1986).

16. de Miro, M. *Acta Geol. Hisp.* **4,** 102–108 (1971).
17. Leyden, B. W. *Proc. nat. Sci.* **81,** 4856–4859 (1984).
18. Bradbury, J. P. *et al. Science* **214,** 1299–1305 (1981).
19. Binford, M. W. *Ecol. Monogr.* **52,** 307–333 (1982).
20. Watts, W. A. & Stuiver, M. *Science* **210,** 325–327 (1980).
21. Autin, W. J., Burns, S. F., Miller, B. J., Saucier, R. T. & Snead, J. I. in *Quaternary Non-Glacial Geology of the Conterminous United States* (ed. Morrison, R. B.) (Geological Society of America, Boulder, in the press).
22. Saucier, R. T. & Fleetwood, A. R. *Geol. Soc. Am. Bull.* **81,** 869–890 (1970).
23. Watts, W. A. in *Late -Quaternary Environments of the United States, Vol. 1, The Late Pleistocene* (ed. Porter, S. C.) 294–310 (University of Minnesota Press, Minneapolis, 1983).
24. Watts, W. A. *Geology* **3,** 344–346 (1975).
25. Watts, W. A. *Quat. Res.* **13,** 187–199 (1980).
26. Watts, W. A. *Geol. Soc. Am. Bull.* **86,** 287–291 (1975).
27. Watts, W. A. *Ecology* **51,** 17–33 (1970).
28. Oglesby, R. J., Maasch, K. A. & Saltzman, B. *Clim. Dyn.* (in the press).
29. Keigwin, L. & Jones, G. *Am. Quat. Ass. Prog. Abstr.* **10,** 24–26 (1988).
30. Prell, W. L. & Hays, J. D. *Mem. geol. Soc. Am.* **145,** 201–220 (1976).
31. Oppo, D. W. & Fairbanks, R. G. *Earth planet. Sci. Lett.* **86,** 1–15 (1987).
32. Hansen, J. *et al. Mon. Weath. Rev.* **3,** 609–662 (1983).
33. Kennett, J. P. & Huddlestun, P. *Quat. Res.* **2,** 384–395 (1972).
34. Brunner, C. A. *Quat. Res.* **17,** 105–119 (1982).
35. Brooks, D. A. & Legeckis, R. V. *J. geophys. Res.* **87,** 4195–4206 (1982).
36. Hastenrath, S. & Kutzbach, J. E. *Quat. Res.* **24,** 249–256 (1985).
37. Showers, W. J. & Bevis, M. *Palaeogeogr., Palaeoclimatol., Palaeoecol.* **64,** 189–199 (1988).
38. Butzer, K. W., Isaac, G. L., Richardson, J. L. & Washbourn-Kamau, C. *Science* **175,** 1069–1076 (1972).
39. Street-Perrott, F. A. & Roberts, N. in *Variations in the Global Water Budget* (eds Street-Perrott, A., Beran, M. & Ratcliffe, R.) 331–345 (Reidel, Dordrecht, 1983).
40. Talbot, M. R. & Delibrias, G. *Earth planet. Sci. Lett.* **47,** 336–344 (1980).
41. Gillespie, R., Street-Perrott, F. A. & Switsur, R. *Nature* **306,** 680–683 (1983).
42. Rognon, P. in *Abrupt Climatic Change—Evidence and Implications* (eds Berger, W. H. & Labeyrie, L. D.) 209–220 (Reidel, Dordrecht, 1987).
43. Sarnthein, M. *Nature* **272,** 43–45 (1978).
44. Rossignol-Strick, M. & Duzer, D. *Met. Forsch.-Erge.* **30,** 1–14 (1979).
45. Pokras, E. M. & Mix, A. C. *Quat. Res.* **24,** 137–149 (1985).
46. Pastouret, L., Chamley, H., Delibrias, G., Duplessy, J. C. & Thiede, J. *Oceanol. Acta* **1,** 217–232 (1978).
47. Patterson, W. S. B. & Hammer, C. U. in *North America and Adjacent Oceans During the Last Deglaciation* (eds Ruddiman, W. F. & Wright, H. E. Jr) 91–109 (Geological Society of America, Boulder, 1987).
48. Mix, A. C., Ruddiman, W. F. & McIntyre, A. *Paleoceanography* **1,** 43–66 (1986).
49. Denton, G. H. & Hughes, T. S. *The Last Great Ice Sheets* (Wiley, New York, 1980).
50. Berger, A. J. *J. atmos. Sci.* **35,** 2362–2367 (1978).
51. CLIMAP Project Members *Geol. Soc. Am. Map Chart Ser.* MC-36 (1981).

ACKNOWLEDGEMENTS. We thank W. Ruddiman, A. McIntyre, W. Prell, B. Molfino, T. Webb III, R. Saucier, W. Broecker, P. McDowell, J. Cole, R. Webb, E. Pokras, S. Jackson, B. Leyden, D. Peteet, D. Murray, D. Olson and C. Rooth for discussions and comments on our manuscript. This work was supported by the NSF Climate Dynamics Program and NASA.

Identification of angiogenic activity and the cloning and expression of platelet-derived endothelial cell growth factor

Fuyuki Ishikawa*, Kohei Miyazono*†, Ulf Hellman†, Hannes Drexler‡, Christer Wernstedt†, Koichi Hagiwara*, Kensuke Usuki†, Fumimaro Takaku*, Werner Risau‡ & Carl-Henrik Heldin†§

* The Third Department of Internal Medicine, Faculty of Medicine, University of Tokyo, Hongo, Bunkyo-ku, Tokyo 113, Japan
† Ludwig Institute for Cancer Research, Box 595, Biomedical Center, S-751 23 Uppsala, Sweden
‡ Max-Planck-Institute für Psychiatrie, Am Klopferspitz 18A D-8033 Martinsried, FRG

Cloning and sequencing of the complementary DNA for platelet-derived endothelial cell growth factor indicates that it is a novel factor distinct from previously characterized proteins. The factor, a protein with a relative molecular mass of about 45,000, stimulates endothelial cell growth and chemotaxis *in vitro* and angiogenesis *in vivo*.

PLATELET-DERIVED endothelial cell growth factor (PD-ECGF) is an endothelial cell mitogen of relative molecular mass (M_r) ~ 45,000 (45K) purified to homogeneity from human platelets[1,2]. By contrast with other endothelial mitogens of the fibroblast growth factor (FGF) family (reviewed in refs 3 and 4), PD-ECGF, which seems to be the only endothelial cell growth factor in human platelets[2], does not bind to heparin and does not stimulate the proliferation of fibroblasts[1]. We describe here the protein sequencing, cDNA cloning and expression of functionally active PD-ECGF. In addition, we show that PD-ECGF has chemotactic activity for endothelial cells *in vitro* and angiogenic activity *in vivo*.

Sequence of PD-ECGF

Information about the protein sequence of PD-ECGF was obtained by the N-terminal sequencing of intact PD-ECGF, and by analysing the fragments obtained after digestion with trypsin, staphylococcal V8 protease, or CNBr (Fig. 2).

To localize a source of production of PD-ECGF, a specific antiserum against PD-ECGF (ref. 2) was used to screen cell lines and tissues by immunoblotting. A strong 45K band was found when extract from a term placenta was analysed (data now shown). A cDNA library was therefore constructed in λgt10 using poly(A)$^+$ RNA from human placenta, and screened with oligonucleotide probes constructed using the information from the protein sequencing; the screening of 3×10^5 clones yielded three positive clones.

Nucleotide sequencing of the 1.8-kilobase (kb) insert of one of the clones (λPL8) revealed a short GC-rich 5′ untranslated region, an open reading frame predicting the translation of a 482-residue protein (M_r 49,972), and a short 3′ untranslated sequence containing a poly(A)$^+$ tail (Fig. 1). The translation is probably initiated by the ATG start codon at nucleotides 124–126, as the surrounding nucleotide sequence follows the rules for translation initiation[5], whereas the sequence surrounding ATG at nucleotides 136–138 does not. Furthermore, there are no other ATG codons between an in-frame stop codon at nucleotides 28–30 and the nucleotides coding for the N-terminus of intact PD-ECGF (Fig. 2). A stop codon (TAA) is present at nucleotides 1,570–1,572, and is part of the polyadenylation signal (nucleotides 1,568–1,573). Fourteen nucleotides downstream of this signal, a long stretch of poly(A)$^+$ was found. A similar overlap of the stop codon and the polyadenylation signal has been reported for human choriogonadotropin B-chain[6].

Of the 482 amino-acids of PD-ECGF deduced from the cDNA clone, 389 were identified by amino-acid sequencing (Fig. 2). The N-terminal sequence of PD-ECGF starts 10 amino acids downstream of the proposed translation initiation site, indicating that the molecule undergoes a limited proteolytic processing after synthesis. The C-terminal amino acids predicted from the

§ To whom correspondence should be addressed.